

# Iterative McCormick Relaxation for Joint Impedance Control and Network Topology Optimization

Junseon Park<sup>\*,§</sup>, Hyeonon Park<sup>\*</sup>, Rahul K. Gupta<sup>§</sup>

<sup>\*</sup>Pukyong National University, Busan, South Korea, <sup>§</sup>Washington State University, Pullman, WA, USA.

Abstract—Power system operators are increasingly deploying Variable Impedance Devices (VIDs), e.g., Smart Wires, and Network Topology Optimization (NTO) schemes for mitigating operational challenges such as line and transformer congestion, and voltage violations. This work aims to optimize and coordinate the operation of distributed VIDs considering fixed and optimized topologies. This problem is inherently non-linear due to power flow equations as well as bilinear terms introduced due to variable line impedance of VIDs. Furthermore, the topology optimization scheme makes it a mixed integer nonlinear problem. To tackle this, we introduce using McCormick relaxation scheme, which converts the bilinear constraints into a linear set of constraints along with the DC power flow equations. We propose an iterative correction of the McCormick relaxation to enhance its accuracy. The proposed framework is validated on standard IEEE benchmark test systems, and we present a performance comparison of the iterative McCormick method against the non-linear, SOS2 piecewise linear approximation, and original McCormick relaxation.

Index Terms—McCormick relaxation, Impedance controller, Network topology optimization, Optimal power flow.

## I. Introduction

The power system is facing operational challenges such as power flow congestion and voltage quality issues [1], [2] due to massive interconnection of intermittent renewable energy resources (RERs), inverter-based resources (IBRs) [3] as well as data center loads [4]. On the one hand, utilities are looking for different long-term solutions such as network expansion, transformer upgrade [5], etc. On the other hand, several Grid Enhancing Technologies (GETs) have emerged as promising alternatives to improve network flexibility and mitigate congestion issues [6]. These include Network Topology Optimization (NTO) [7], Variable Impedance Devices (VIDs), also referred to as Smart Wire Devices (SWDs) [8], etc.

Prior work has demonstrated that NTO can significantly reduce operational costs relative to fixed-topology systems [7], and improve operational flexibility. In contrast, VIDs, or SWDs, dynamically adjust line impedance to redistribute power flows from congested to lightly loaded transmission lines [8]. VIDs are a type of flexible AC transmission system (FACTS), such as Thyristor Controlled Series Compensator (TCSC), Static Synchronous Series Compensator (SSSC), Unified Power Flow Controller (UPFC), etc., and can be modeled by variable line impedance. The variable impedance/reactance allows flexibility in the transmission network to re-route the power flows and help avoid congestion and reduce costs.

In the existing literature, the optimization of distributed VIDs across has been widely investigated. Incorporating VIDs into operational planning introduces additional nonlinearities in both the optimal power flow (OPF) and switching problems, as VIDs are typically modeled through variable line impedance [8], [9]. Different methods have been proposed to tackle the nonlinearities. For example, the work in [8] proposes a mixed integer reformulation; however, the controls are limited to the maximum and minimum operation setpoints of the VIDs. A similar strategy was used in [9] for the placement of the SWDs to facilitate integration of large-scale wind power plants. Overall, these methods are focused on the planning of the SWDs. The work in [10] developed a scheme for the operation of SWDs using a sensitivity factor approach, but they are not applicable to different topologies.

In this work, we focus on the joint optimal operation of the VIDs with base and optimized topology. First, the network topology and bus-bar splitting are modeled using the node-breaker representation, which enables detailed switching decisions while maintaining network connectivity and operational feasibility. Then, VIDs are incorporated to provide additional flexibility by allowing controlled adjustments of line reactances within predefined operating limits, thereby redistributing power flows and alleviating congestion. The DC power flow model is adopted to represent power flow physics, extended to account for the variable line reactances introduced by the VIDs.

As this problem has bilinear constraints, we propose a McCormick relaxation-based approach to linearize the bilinear constraints in the DC-OPF and NTO problems. However, this scheme usually results in large errors due to the McCormick relaxation, especially when the allowable change in the network impedance is large, for example, 30-50% of the rated value. For enhancing the accuracy of the McCormick relaxation approach, we propose an iterative McCormick method, where the bounds on the maximum allowable range in the impedance is changed in steps. The key contribution of this work lies in linearization techniques using the iterative McCormick relaxation approach and its performance comparison with respect to the nonlinear and mixed integer schemes.

The paper is organized as follows. Section II presents the problem formulation. Section III presents the relaxation using the McCormick method and SOS2 approximation. Section IV presents the simulation setup and results on

different IEEE testcases, and finally, Section V concludes the main contribution of the presented work.

## II. Problem Formulation

We consider a power transmission network consisting of  $N_b$  buses,  $N_g$  generators and connected with several VIDs. The objective is to optimize the operation of generators, load-shedding, distributed VIDs and the network topology. The optimization objectives and the constraints are defined below.

### A. Objective function

The proposed optimization aims to minimize the total system operating cost, which consists of (i) generation cost ( $C^{Gen}$ ) and (ii) load-shedding cost ( $C^{LS}$ ), defined as follows.

1) Generation cost: They are modeled as a quadratic function, as shown in Equation (1a), where the net generation is the sum of the generation produced at the two busbars.

$$C^{Gen} = \sum_{g=1}^{N_g} (c_{g,2}(P_{g,1} + P_{g,2})^2 + c_{g,1}(P_{g,1} + P_{g,2}) + c_{g,0}) \quad (1a)$$

where,  $c_{g,0}$ ,  $c_{g,1}$  and  $c_{g,2}$  are the cost parameters of the generators and  $P_{g,1}$  and  $P_{g,2}$  refer to the generator units at busbar 1 and 2, respectively.

2) Load shedding cost: When transmission capacity constraints fail to meet the total load demand, load shedding may occur. Multiplying the load shedding power by a high-cost  $VOLL$  minimizes the load shedding cost. The load shedding cost can be calculated as shown in Equation (1b).

$$C^{LS} = VOLL \sum_{b=1}^{N_b} \left( \sum_{d \in D_b} (P_{b,d}^{max} - (P_{b,d,1} + P_{b,d,2})) \right) \quad (1b)$$

where,  $VOLL$  refers to the value of loss of load,  $P_{b,d,1}$  and  $P_{b,d,2}$  are the demand at busbars 1 and 2 of bus  $b$ . The symbol  $P_{b,d}^{max}$  refer to the maximum demand at bus  $b$ .  $D_b$  represents a set containing the indices of the demand per bus  $b$ .

### B. Constraints

The constraint set consists of a power flow model, constraints on the network topology, constraints on the generators and load-shedding. These are described below.

1) Transmission Grid Model: We model the transmission network using the DC power flow approximation [11], which assumes that (i) the angle of the voltage difference is small, (ii) the network is reactive, and (iii) the voltage magnitudes are close to 1 per unit. Let the symbol  $b_l$  represent the susceptance of line  $l$ ,  $\theta_{l,fr}$  and  $\theta_{l,to}$  denote the voltage angle for line  $l$  at "from" and "to" ends. Then, the flow in line  $l$ ,  $P_l$  can be expressed using DC power flow model as

$$P_l = b_l(\theta_{l,fr} - \theta_{l,to}). \quad (2)$$

2) Network Topology Optimization Model: NTO identifies optimal network topology by utilizing controllable switching devices, including transmission switches and substation circuit breakers (CBs). Substation CBs enable reconfiguration of internal bus arrangements and their interfaces with the rest of the network, thereby affecting grid flexibility, reliability, and security. Various bus configurations are used in practice, each requiring different numbers of breakers and offering distinct reliability characteristics; among them, the breaker-and-a-half scheme is common in high-voltage substations due to its favorable balance of reliability and operational flexibility [12]. In this work, we modeled the substations using the node-breaker (NB) representation. Figure 1 shows a generalized breaker-and-a-half layout with line-switching capability. This NB model provides additional reconfiguration options, allowing the "from" and "to" busbars to be opened or closed independently and enabling loads and generators to connect to either busbar.

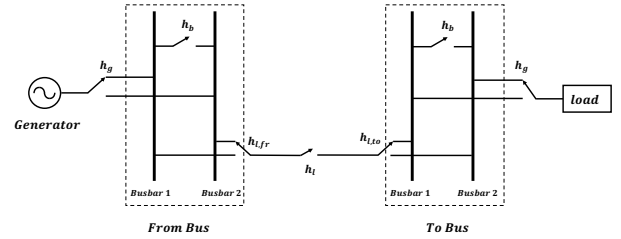


Fig. 1. Generalized breaker-and-a-half model.

Considering the switching capability of the busbars and the lines, the NTO model can be mathematically modeled using busbar binary variables  $h_b$  [7], [13]:

$$-\theta^{max}(1 - h_b) \leq \theta_{b,1} - \theta_{b,2} \leq \theta^{max}(1 - h_b) \quad \forall b, \quad (3a)$$

where  $\theta_{b,1}$  and  $\theta_{b,2}$  are the voltage angles at busbars 1 and 2 and  $\theta^{max}$  is the maximum difference of angle between the busbars. In (3a), when busbars are merged, the difference in voltage angle phase between busbars must be identical, and when split, it must not exceed the maximum angle phase.

The generators connected at each busbar can be modeled using binary variables  $h_g$ , and can be expressed as

$$(1 - h_g)P_g^{min} \leq P_{g,1} \leq (1 - h_g)P_g^{max} \quad \forall g \quad (3b)$$

$$h_g P_g^{min} \leq P_{g,2} \leq h_g P_g^{max} \quad \forall g. \quad (3c)$$

The symbols  $P_g^{min}$  and  $P_g^{max}$  denote the minimum and maximum limits. Eqs. (3b) and (3c) model when a generator is connected to busbar 1 or at busbar 2, and vice versa.

Similarly, the connection and controllability of the demand at each of the busbars are modeled using binary variable  $h_d$  using (3d) and bounded by (3e)

$$0 \leq P_{b,d,1} \leq (1 - h_d)P_{b,d}^{max} \quad \forall b \quad (3d)$$

$$0 \leq P_{b,d,2} \leq h_d P_{b,d}^{max} \quad \forall b. \quad (3e)$$

The limit on the power-flow for each line and the switching of the lines are expressed as

$$-(1 - h_{l,e})P_l^{max} \leq P_{l,e,1} \leq (1 - h_{l,e})P_l^{max} \quad \forall l, e \quad (3f)$$

$$-h_{l,e}P_l^{max} \leq P_{l,e,2} \leq h_{l,e}P_l^{max} \quad \forall l, e \quad (3g)$$

$$-h_l P_l^{max} \leq P_{l,e,1} \leq h_l P_l^{max} \quad \forall l, e \quad (3h)$$

$$h_{l,e} \leq h_l \quad \forall l, e \quad (3i)$$

$$P_l = P_{l,e,1} + P_{l,e,2} \quad \forall l, e \quad (3j)$$

where  $h_{l,e}$  refer to binary variable representing whether line  $l$  is on or off.  $e = \{\text{"from"}, \text{"to"}\}$  refer to the ends of the line.  $P_l^{max}$  defines the maximum capacity of line  $l$ .  $P_{l,e,1}$  and  $P_{l,e,2}$  refer to power flow of line  $l$  at the end side of  $e$  through busbar 1 and busbar 2 respectively. Eqs. (3f) and (3g) define the transmission line constraints: when a line is connected to busbar 1, the power flow to the other busbars must be zero, and vice versa. Eqs. (3h) and (3i) specify the line status, ensuring that no power flows when the line is open. Constraint (3j) enforces power conservation by requiring that the total power flowing out of a busbar equals the power flowing from the 'from' bus to the 'to' bus.

The line switching constraints are expressed using the big- $M$  method, given by (3k), (3l), and (3m)

$$-M(1 - h_l) \leq b_l(\theta_{l,fr} - \theta_{l,to}) - P_l \leq M(1 - h_l) \quad \forall l \quad (3k)$$

$$-h_{l,e}\theta^{max} \leq \theta_{l,e} - \theta_{l,e,1} \leq h_{l,e}\theta^{max} \quad \forall l, e \quad (3l)$$

$$-(1 - h_{l,e}\theta^{max}) \leq \theta_{l,e} - \theta_{l,e,2} \leq h_{l,e}\theta^{max} \quad \forall l, e. \quad (3m)$$

The binary variables for busbars, generators, demand connections, and lines are connected through Eqs. (3n), (3o), and (3p). When the busbars at each substation are connected, it is not necessary to consider the binary variable determining the connection of the generator, load, and end of the line.

$$h_b + h_g \leq 1 \quad \forall b, g \in G_b \quad (3n)$$

$$h_b + h_d \leq 1 \quad \forall b, d \in D_b \quad (3o)$$

$$h_b + h_{l,e} \leq 1 \quad \forall b, e, l \in LF_b \text{ or } l \in LT_b. \quad (3p)$$

Finally, the constraints (3q) and (3r) express the power balance constraints, i.e., the difference between generation and demand is equal to the sum of power flowing through the lines. The symbol  $G_b$  refers to a set containing the indices of the generator per bus  $b$ .  $LF_b$  and  $LT_b$  denote set of lines flow "from" bus  $b$  and "to" bus  $b$ , respectively.

$$\sum_{g \in G_b} P_{g,1} - \sum_{d \in D_b} P_{b,d,1} - \sum_{l \in LF_b} P_l + \sum_{l \in LT_b} P_l = 0 \quad \forall b \quad (3q)$$

$$\sum_{g \in G_b} P_{g,2} - \sum_{d \in D_b} P_{b,d,2} - \sum_{l \in LF_b} P_l + \sum_{l \in LT_b} P_l = 0 \quad \forall b \quad (3r)$$

3) VID Model: VIDs can be mathematically modeled as variable susceptance devices [8], [9], [14] as

$$b_l = \bar{b}_l + \Delta b_l \quad (4a)$$

$$-r\bar{b}_l \leq \Delta b_l \leq r\bar{b}_l \quad \forall l \quad (4b)$$

where,  $\bar{b}_l$  denotes the nominal susceptance and  $\Delta b_l$  is a variable allowing deviations in the line susceptance is bounded by a factor  $r \leq 1$  of nominal susceptance  $\bar{b}_l$ .

### C. Final Optimization Problem

The final optimization can be formulated as

$$\begin{aligned} \min \quad & C^{Obj} = C^{Gen} + C^{LS}, \\ \text{subject to} \quad & (3), (4). \end{aligned} \quad (5)$$

Note that the optimization problem in (5) is non-linear because of the bilinear variables  $\Delta b_l(\theta_{l,fr} - \theta_{l,to})$  due to VIDs when (4) is substituted in (3k) and (2) with  $\Delta b_l$  and  $\theta_{l,fr}, \theta_{l,to}$  being variables. Therefore, we propose a linearization approach using McCormick Relaxation as described below.

## III. McCormick Relaxation and SOS2 Approximation

### A. McCormick Relaxation Model

1) McCormick Relaxation (Non-iterative): We relax bilinear terms,  $\Delta b_l(\theta_{l,fr} - \theta_{l,to})$ , by defining auxiliary variables, then applying McCormick envelopes [15]. These McCormick envelopes transform the bilinear constraints to a set of linear constraints by defining upper and lower bounds on each of the variables in the bilinear term. We define upper and lower bounds on the variables involved in the bilinear constraint, i.e.,  $[b_l^{min}, b_l^{max}]$  and  $[\Delta\theta_l^{min}, \Delta\theta_l^{max}]$ , then the McCormick constraint set is defined as follows. We define a new variable  $w_l = \Delta b_l \Delta\theta_l$  where  $\Delta\theta_l = \theta_{l,fr} - \theta_{l,to}$ . Then, the McCormick relaxation is given as (6a)-(6d):

$$w_l \geq b_l^{min} \Delta\theta_l + \Delta b_l \Delta\theta_l^{min} - b_l^{min} \Delta\theta_l^{min} \quad \forall l \quad (6a)$$

$$w_l \geq b_l^{max} \Delta\theta_l + \Delta b_l \Delta\theta_l^{max} - b_l^{max} \Delta\theta_l^{max} \quad \forall l \quad (6b)$$

$$w_l \leq b_l^{min} \Delta\theta_l + \Delta b_l \Delta\theta_l^{max} - b_l^{min} \Delta\theta_l^{max} \quad \forall l \quad (6c)$$

$$w_l \leq b_l^{max} \Delta\theta_l + \Delta b_l \Delta\theta_l^{min} - b_l^{max} \Delta\theta_l^{min} \quad \forall l. \quad (6d)$$

2) Iterative McCormick Relaxation: The accuracy of the McCormick relaxation scheme is strongly influenced by the range of bounds associated with the variables in the McCormick equations. As it will be demonstrated in the Results section, the objectives obtained using the McCormick relaxation method exhibit a deviation from the costs computed by a nonlinear solver. To address this discrepancy, we propose an iterative McCormick relaxation technique, formally described in Algorithm 1. This algorithm applies McCormick relaxation in small steps, so that the accuracy is not compromised.

---

**Algorithm 1** Iterative McCormick Relaxation with Incremental  $r$  Updates

---

Require: Target relaxation level  $r_{\text{final}}$ , step size  $\Delta r$ , initial susceptances  $\{b_l\}$

- 1: Initialize  $\hat{b}_l \leftarrow b_l$  for all lines  $l$
- 2: while  $r < r_{\text{final}}$  do
- 3:   Solve (5) using McCormick relaxation (6) for  $r = \Delta r$
- 4:   Compute susceptance update  $\Delta b_l$
- 5:   Update susceptance:  $\hat{b}_l \leftarrow b_l + \Delta b_l$  for all  $l$
- 6:    $r \leftarrow r + \Delta r$
- 7: end while
- 8: return final solution at  $r_{\text{final}}$

---

### B. SOS2 Model

The bilinear term  $b_l \Delta \theta_l$  in (2) and (3k) can also be approximated by a two-dimensional piecewise-linear model using special ordered sets of type 2 (SOS2). For each line  $l$ , the range  $[b_l^{\min}, b_l^{\max}]$  and  $[\Delta \theta_l^{\min}, \Delta \theta_l^{\max}]$  are divided into  $N_b^{\text{grid}}$  and  $N_\theta^{\text{grid}}$  number of interpolation points, denoted by  $\hat{b}_{l,i}$  and  $\widehat{\Delta \theta}_{l,j}$ . SOS2 constraints are constructed by defining continuous variables  $\lambda_{l,i,j}, \alpha_{l,i}, \beta_{l,j}$  such that

$$\sum_{i=1}^{N_b^{\text{grid}}} \sum_{j=1}^{N_\theta^{\text{grid}}} \lambda_{l,i,j} = 1; \quad \alpha_{l,i} = \sum_j \lambda_{l,i,j}; \quad \beta_{l,j} = \sum_i \lambda_{l,i,j}. \quad (7a)$$

The vectors  $(\alpha_{l,1}, \dots, \alpha_{l,N_b^{\text{grid}}})$  and  $(\beta_{l,1}, \dots, \beta_{l,N_\theta^{\text{grid}}})$  are modeled as SOS2 sets, ensuring that only two adjacent breakpoints are active along each axis. In our implementation,  $\lambda_{l,i,j}$ ,  $\alpha_{l,i}$ , and  $\beta_{l,j}$  are modeled as continuous variables, while the adjacency structure of the piecewise-linear model is imposed through the SOS2 constraints; YALMIP<sup>1</sup> creates an SOS2 set and automatically adds the binary variables and linear constraints required to enforce the adjacency structure.

Using the interpolation weights, the line susceptance, angle difference, and an auxiliary variable  $\tilde{w}_l$  that approximates the product  $b_l \Delta \theta_l$  are defined as

$$b_l = \sum_{i,j} \lambda_{l,i,j} \hat{b}_{l,i}, \quad \Delta \theta_l = \sum_{i,j} \lambda_{l,i,j} \widehat{\Delta \theta}_{l,j}, \quad (8a)$$

$$\tilde{w}_l = \sum_{i,j} \lambda_{l,i,j} \hat{b}_{l,i} \widehat{\Delta \theta}_{l,j}. \quad (8b)$$

Finally, the SOS2 approximation replaces the bilinear flow relation in (3k) through

$$-M(1 - h_l) \leq \tilde{w}_l - P_l \leq M(1 - h_l), \quad (9a)$$

$$-P_l^{\max} \leq P_l \leq P_l^{\max}, \quad (9b)$$

where  $M$  is a sufficiently large constant. When  $h_l = 1$ , (9a) enforces  $P_l = \tilde{w}_l$ , yielding a piecewise-linear approximation of  $b_l \Delta \theta_l$ . When  $h_l = 0$ , the constraint is relaxed, and the line flow is handled through the NTO constraints in (3).

<sup>1</sup><https://yalmip.github.io/command/sos2/>

## IV. Numerical Simulations

### A. Simulation Setup

We simulate our framework on four different IEEE benchmark test systems, which are Case300, Case588\_sdet, Case1354pegase, and Case1888rte [16], and will be described in the results section. We used the dataset from the MATPOWER testcases for the simulations.

For each testcase, we set the minimum output of all generators to zero in order to avoid situations where a generator's minimum output would exceed the load at its corresponding bus. To simulate the congestion scenario, where the control of VIDs and NTO would be beneficial, we artificially reduce the capacity of the transmission lines. This is done by first solve the OPF for the nominal case, then we set the capacity of the lines to be 80% of the power-flows obtained in the nominal case. For the simulations with VIDs, we allow the susceptance change factor (4b),  $r$  is set from 0 to 0.5, allowing each line susceptance to vary up to 50% of their nominal values. The cost of load shedding (VOLL) is set to 2,000 \$/MWh.

### B. Results

The results of the proposed iterative-McCormick relaxation is presented and compared against three different formulations: Nonlinear, McCormick, and SOS2. The performance are compared with respect to the achieved cost, computation time, and accuracy with respect to the nonlinear case. We use Gurobi 12.0<sup>2</sup> as the optimization solver for all the cases.

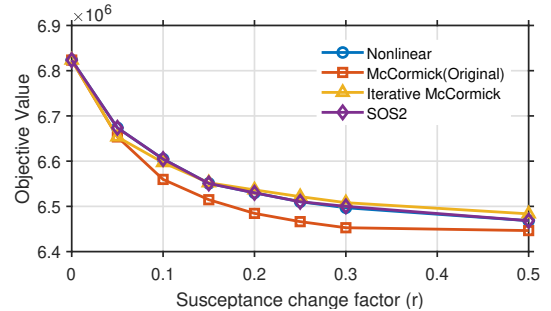


Fig. 2. Performance comparison of objective function costs under different methods for Case300 using the nominal topology.

TABLE I  
Error and computation time of relaxation/approx methods for different  $r$  (Case300, Nominal Topology)

$r$ (%)	Nonlinear	McCormick (Original)		Iterative McCormick		SOS2	
	Time (s)	Error (%)	Time (s)	Error (%)	Time (s)	Error (%)	Time (s)
0	1.18	0.000	1.05	0.000	1.06	0.000	1.80
5	1.76	0.300	1.11	0.300	1.07	0.001	6.78
10	1.91	0.681	1.10	0.117	2.13	0.000	12.42
15	1.99	0.550	1.11	0.021	3.19	0.000	8.40
20	2.07	0.697	1.10	0.099	4.21	0.000	31.03
25	2.16	0.677	1.11	0.173	5.24	0.000	31.82
30	2.07	0.680	1.10	0.172	6.34	0.047	6.98
50	1.95	0.338	1.11	0.234	10.59	0.000	9.53

<sup>2</sup><https://www.gurobi.com>

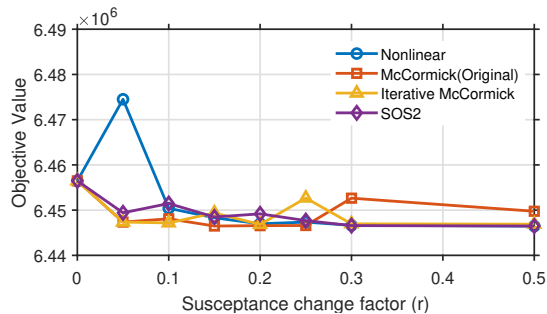


Fig. 3. Performance comparison of objective function costs under different methods for Case300 using the optimal topology via NTO.

TABLE II

Error and computation time of relaxation/approx methods for different  $r$  (Case300, Optimal Topology using NTO)

$r$ (%)	Nonlinear		McCormick (Original)		Iterative McCormick		SOS2	
	Time (s)	Error (%)	Time (s)	Error (%)	Time (s)	Error (%)	Time (s)	
0	1205.93 <sup>†</sup>	0.000	1205.33 <sup>†</sup>	0.000	1205.69 <sup>†</sup>	0.000	1205.54 <sup>†</sup>	
5	1206.95 <sup>†</sup>	0.419	81.97	0.419	78.55	0.388	179.80	
10	920.84	0.036	41.42	0.050	128.78	0.016	47.61	
15	564.82	0.028	15.53	0.017	185.17	0.003	46.16	
20	375.47	0.006	22.66	0.002	246.85	0.034	135.91	
25	435.44	0.012	22.39	0.082	312.15	0.005	112.66	
30	342.35	0.093	20.10	0.005	365.00	0.001	75.62	
50	151.38	0.051	32.76	0.006	544.09	0.000	44.16	

<sup>†</sup>Indicates instances that reached the 1200s time limit. At  $r = 0\%$ , all methods reached the limit; at  $r = 5\%$ , only the nonlinear formulation did.

1) Case300 System: The optimized objectives using the nonlinear, McCormick, iterative-McCormick, and SOS2 are shown in Fig. 2. From the plot, we can make two observations. First, the cost goes down with an increase in  $r$  i.e., the flexibility in changing the line susceptance thanks to VIDs. Second, the iterative McCormick and SOS2 costs are quite close to the nonlinear case, whereas the original McCormick deviates from the nonlinear cost as  $r$  increases. This happens because an increase in  $r$  leads to a larger McCormick relaxation and therefore it is more inexact.

We also quantify the difference between the costs obtained by relaxed and approximated methods with respect to the nonlinear method in Table I. It also shows the computation time for each method. It shows that the iterative McCormick method improves upon the error, but it takes more time due to the iterations. For this case, SOS2 performs the best both in terms of time and accuracy.

The results with optimized topology, i.e., solving the NTO problem with VIDs, are shown in Fig 3. Here, we see that the cost does not change much with an increase in  $r$ , this is because NTO already reduced the cost by a large margin, and there is not much improvement that can be achieved using VIDs for this testcase. In some cases, the value of the cost function increases as the  $r$  increases. This is because the Gurobi solver's Gap was set to 0.1%, leading to errors. The error is especially large when  $r$  is 5% between the Nonlinear model and the other models. This is caused by the solver not converging to a solution within the time limit (1200 seconds). The error and computation time are presented in Table II. We again observed that SOS2 is the best-performing approximation.

2) Larger testcases: To evaluate whether the proposed scheme is scalable on larger networks, we simulate it for Case588\_sdet, Case1354pegase, and Case1888rte. For brevity, we present the result for  $r = 10\%$  considering the nominal topology. The results are presented in Table III comparing the cost, computation time, and accuracy. We observe that the proposed iterative McCormick achieves the best performance in accuracy and computation time for all the larger systems.

## V. Conclusions

This work considered the problem of optimizing the operation of distributed variable impedance devices with network topology optimization in power transmission networks. Due to the varying nature of the line reactances, this problem contained bilinear constraints. The work proposed using McCormick envelopes to relax the bilinear constraints, which results in a large error compared to the objective obtained by the nonlinear model. Therefore, we proposed an iterative approach to apply McCormick envelopes in small steps. The proposed method was compared against the nonlinear method, the original McCormick relaxation, and the SOS2 approximation. The comparison was performed with respect to the error against the nonlinear method and the computation time. We observe that the proposed method performs the best on large systems such as Case588\_sdet, Case1354pegase, and Case1888rte, whereas for the smaller networks, e.g., case300, SOS2 performs the best. Future work will focus on using the proposed scheme for optimal planning of variable impedance devices in the transmission system.

## References

- [1] X. Liang, "Emerging power quality challenges due to integration of renewable energy sources," *IEEE Transactions on Industry Applications*, vol. 53, no. 2, pp. 855–866, 2016.
- [2] North American Electric Reliability Corporation., "Characteristics and risks of emerging large loads - large loads task force white paper," July, 2025. [Online]. Available: [https://www.nerc.com/comm/RSTC\\_Reliability\\_Guidelines/Whitepaper%20Characteristics%20and%20Risks%20of%20Emerging%20Large%20Loads.pdf](https://www.nerc.com/comm/RSTC_Reliability_Guidelines/Whitepaper%20Characteristics%20and%20Risks%20of%20Emerging%20Large%20Loads.pdf)
- [3] Y. Lin et al., "Pathways to the next-generation power system with inverter-based resources: Challenges and recommendations," *IEEE Electrification Magazine*, vol. 10, no. 1, pp. 10–21, 2022.
- [4] U.S. Department of Energy., "Evaluating the reliability and security of the united states electric grid," July, 2025. [Online]. Available: <https://www.energy.gov/sites/default/files/2025-07/DOE%20Final%20EO%20Report%20%28FINAL%20JULY%207%29.pdf>
- [5] S. De La Torre, A. J. Conejo, and J. Contreras, "Transmission expansion planning in electricity markets," *IEEE transactions on power systems*, vol. 23, no. 1, pp. 238–248, 2008.
- [6] U.S. Department of Energy., "Grid-enhancing technologies: Unlocking the full potential of transmission capacity," 2021. [Online]. Available: <https://www.energy.gov/gdo/grid-enhancing-technologies>
- [7] R. Xiao, Y. Xiang, L. Wang, and K. Xie, "Power system reliability evaluation incorporating dynamic thermal rating and network topology optimization," *IEEE Trans. Power Sys.*, vol. 33, no. 6, pp. 6000–6012, 2018.

TABLE III  
Objective values, error (in parentheses, relative to the nonlinear objective value),  
and computation time for larger testcases using different methods ( $r = 10\%$ ).

IEEE Test bus system	Objective Values (\$)				Computation Time (s)				
	Nonlinear	McCormick (Original)	Iterative McCormick	SOS2	Nonlinear	McCormick (Original)	Iterative McCormick	SOS2	
case300	6,604,576	6,559,597 (0.681%)	6,596,829 (0.117%)	6,604,576 (0.000%)	1.91	1.10	2.13	12.42	
case588_sdet	1,787,169	1,786,860 (0.017%)	1,787,144 (0.001%)	1,787,413 (0.014%)	59.46	2.29	3.79	5.14	
case1354pegase	25,628,319	25,581,370 (0.183%)	25,620,519 (0.03%)	25,635,474 (0.028%)	3473.10	5.07	10.22	24.51	
case1888rte	19,392,895	18,545,441 (4.370%)	18,701,887 (3.563%)	18,729,993 (3.42% <sup>†</sup> )	27850.38	7.85	16.08	14400	

<sup>†</sup>Indicates solution up to 0.26% gap interrupted due to time limit: 4 hours.

- [8] M. Sahraei-Ardakani and K. W. Hedman, "Computationally efficient adjustment of facts set points in dc optimal power flow with shift factor structure," IEEE TPWRS, vol. 32, no. 3, pp. 1733–1740, 2016.
- [9] A. Nikoobakht, J. Aghaei, T. Niknam, M. Shafie-khah, and J. P. Catalao, "Smart wire placement to facilitate large-scale wind energy integration: an adaptive robust approach," IEEE Transactions on Sustainable Energy, vol. 10, no. 4, pp. 1981–1992, 2018.
- [10] O. Pohl, "Coordination of impedance controllers and flexible power for curative congestion management in real-time applications," Ph.D. dissertation, Dissertation, Dortmund, Technische Universität, 2024, 2024.
- [11] B. Stott, J. Jardim, and O. Alsac, "Dc power flow revisited," IEEE Transactions on Power Systems, vol. 24, no. 3, pp. 1290–1300, 2009.
- [12] D. Atanackovic, D. McGillis, and F. Galiana, "Reliability comparison of substation designs," IEEE transactions on power delivery, vol. 14, no. 3, pp. 903–910, 1999.
- [13] M. Heidarifar and H. Ghasemi, "A network topology optimization model based on substation and node-breaker modeling," IEEE Transactions on Power Systems, vol. 31, no. 1, pp. 247–255, 2016.
- [14] O. Pohl, S. Dalhues, and C. Rehtanz, "Dc-sensitivities for impedance controllers in an agent-based power flow control system," in 2018 ISGT, 2018, pp. 1–5.
- [15] A. Mitsos, B. Chachuat, and P. I. Barton, "McCormick-based relaxations of algorithms," SIAM Journal on Optimization, vol. 20, no. 2, pp. 573–601, 2009.
- [16] S. Babaeinejadsarookolaee, A. Birchfield, R. D. Christie, C. Coffrin, C. DeMarco, R. Diao, M. Ferris, S. Fliscounakis, S. Greene, R. Huang et al., "The power grid library for benchmarking ac optimal power flow algorithms," arXiv preprint arXiv:1908.02788, 2019.